

# Calculation of Effective Luminosity for PANDA Experiment

*A.Smirnov, A.Sidorin, D.Krestnikov*  
JINR, Dubna, Russia

## Contents

Introduction .....	2
1. Calculation of the luminosity.....	3
1.1. Mean luminosity.....	4
1.2. Beam parameter variation.....	7
1.3. Short time-scale luminosity variations .....	7
1.4. Effective luminosity .....	9
2. WASA experiment .....	11
2.1. Experimental conditions .....	11
2.2. Comparison of experimental and simulation results .....	12
3. Simulation of PANDA experiment .....	15
Conclusion.....	17
Reference.....	17

## Introduction

In last years at GSI (Germany) the new accelerator complex project FAIR is being realized. One of the most important goals of this project is carrying out an experiment with internal target PANDA [1]. One of way to achieve the design luminosity value is to use a pellet target. However, such target is coming up with the short-scale luminosity variation. Peak to mean luminosity ratio can reach a big value unacceptable for detectors.

A numerical simulation of this experiment is connected to two different time-scale processes. The first one is the short-time process, which describes luminosity variations while one pellet is crossing the beam. This process can be about tenths microsecond long. The long-time process of the beam parameter evolution (particle number, transverse and longitudinal profiles) are defined by the beam losses and equilibrium between the target heating and electron cooling.

While the beam is crossing a pellet target, the transverse scattering of the particles on the nucleus field has place to be. That leads to loses of the particles on the acceptance (single scattering on large angle) and to growing emittance because of the multiple scattering on small angles. Loses of the particle energy due to the target atom ionization lead to the decreasing of the average energy and changing revolution frequency of the beam. Fluctuation of energy loses may bring particles losing on the longitudinal acceptance due to single interaction with a target.

Ionization loses of the average energy are compensated by accelerator gap if RF system is switched on. To avoid a large bunching factor of the beam a non-sinusoidal RF wave (so called burrier bucket system) can be used. An application of the burrier bucket system is planed for the PANDA experiment and it was used at the experiments on COSY storage ring [2].

All things described above can be easily modeled using BETACOOOL code [3]. General goal of the BETACOOOL program is to simulate long term processes (in comparison with the ion revolution period) leading to variation of the ion distribution function in 6 dimensional phase space. In the case of the pellet target simulation the existing algorithm is based on assumption that during one step of the integration a large number of the pellets cross the beam. This algorithm does not take into account short-scale luminosity variations. Such variations can be unacceptable for the PANDA detector, therefore numerical simulation of this effect is of great importance.

At the frame of the PANDA collaboration an additional algorithm was developed and implemented into the BETACOOOL. It calculates luminosity time dependencies at the time scale sufficiently shorter then time that takes a pellet to get through the beam.

For benchmarking of the BETACOOOL algorithms, data from experiment with pellet target WASA at COSY storage ring was used [4]. During the COSY run from June 21 to July 5 2008 a luminosity value and different beam parameters were recorded as functions of time. Modeling of the experiment was made using the BETACOOOL program. The purpose of modeling was a comparison of calculated luminosity variations in the storage ring while every pellet is crossing the beam with experimental data.

## 1. Calculation of the luminosity

The luminosity averaged over a period of time sufficiently longer than the pellet time of flight through the antiproton beam can be expressed similarly to another types of internal targets:

$$\langle L \rangle = \frac{N \rho_{eff}}{T_{rev}}, \quad (1.1)$$

where  $N$  is the antiproton number,  $\rho_{eff}$  is the effective target thickness in Atoms/cm<sup>2</sup> that depends on the pellet flux dimensions and the antiproton beam horizontal size. Under assumption of Gaussian distribution of the antiprotons and treating the pellet target as a uniform medium one can calculate the mean luminosity analytically. Such method is usually used for estimation of the required pellet dimensions and the pellet flux parameters.

In the case of arbitrary distribution of antiprotons the luminosity can be calculated using multi particle tracking procedure, as it realized, for example, in the Betacool program. For each modeling particle one can calculate a number of the events when the particle hits the pellet  $N_{cross}$  during a period of time  $\Delta t$ . The luminosity providing by this particle is equal to

$$L_i = \frac{N_{cross} \rho_{pellet}}{\Delta t}, \quad (1.2)$$

where  $\rho_{pellet}$  is the pellet thickness. The pellet thickness is calculated from the pellet density  $\mathfrak{R}$  in Atoms/cm<sup>3</sup> as the integral along the particle trajectory:

$$\rho_{pellet} = \int \mathfrak{R} ds, \quad (1.3)$$

and for spherical shape of the pellet the averaged value over large number of crossings is equal to  $\sqrt{\pi/6} \mathfrak{R} d_p$ , where  $d_p$  is the pellet diameter. The total luminosity is a sum of the luminosities of the individual particles, at  $N_{MP}$  modeling particles it is equal to

$$\langle L \rangle = \frac{N}{N_{MP}} \sum_{i=1}^{N_{MP}} L_i. \quad (1.4)$$

Main difference of the pellet target in comparison with other types of internal targets is its well pronounced granularity. In experiment with a pellet target the luminosity fluctuates from zero (when no pellet is inside the beam) to some maximum value corresponding to the pellet location inside the beam center. The peak luminosity can exceed the mean value (1.1) by a few times. The event rate  $\bar{N}_{event}$  for reaction with a cross-section of  $\sigma$  is connected with the luminosity as

$$\bar{N}_{event} = L \sigma. \quad (1.5)$$

If this value exceeds the maximum count rate, which can provide a detector,  $\bar{N}_{count,max}$ , the detector can saturates (in this case the count rate stays at maximum design value and does not depend on the event rate), or overload (in this case the count rate falls to zero), or some intermediate case can take a place depending on the detector design. The luminosity measured by the detector (or effective luminosity)  $L_{eff}$  is

$$L_{eff} = \frac{\bar{N}_{count}}{\sigma}. \quad (1.6)$$

The short time-scale luminosity variations can be simulated by tracking of individual pellets inside the antiproton beam. The pellet time of flight through the beam is a few  $\mu\text{s}$  and the beam profile is not changed during such a time. The luminosity for each pellet can be calculated as

$$L = \frac{N \int f(x_p, y_p) ds_{\rho_{pellet}}}{T_{rev}}. \quad (1.7)$$

Here  $f(x,y)$  – the normalized antiproton distribution function in the transverse plane,  $x_p, y_p$  are the pellet co-ordinates inside the antiproton beam, the integral is calculated over the pellet cross-section.

Numerical algorithms for long time-scale beam parameter evolution, for short time-scale luminosity variation and for effective luminosity calculation at two models of the detector were realized in the Betacool program. In the current version the antiproton distribution in the transverse plane is calculated in the form of two beam normalized profiles – horizontal and vertical. Brief description of the algorithms is presented in this chapter.

### 1.1. Mean luminosity

To calculate expected number of the pellet crossing during given period of time for the ion at given co-ordinates at the target position in the Betacool is used algorithm based on calculation of crossing probability as a function of the ion Courant-Snyder invariants. The vertical pellet velocity assumed to be so small, that during the time of the pellet motion through the ion beam the ion has a large number of betatron oscillations.

The model of the pellet target is developed on the following basic assumptions.

1. All the pellets have the same size, and the pellet shape can be approximated by box at dimensions  $l \times x_p \times y_p$  at uniform density, which is equal to the density of the frozen gas ( $l$  is the pellet size along the ion trajectory,  $x_p$  and  $y_p$  are the horizontal and vertical sizes). To keep the real density of the pellet the cube dimensions can be recalculated from the pellet diameter  $d$  as  $l = x_p = y_p = d\sqrt[3]{\pi/6}$ .
2. All the pellets move in vertical direction with the same velocity  $v_{pellet}$  and interval between them is equal to  $h$ .
3. Each pellet moves along the straight line shifted in horizontal direction by the distance of  $s$  relatively to the ion beam equilibrium orbit.
4. The pellets form a flux at round shape of horizontal cross-section at radius  $r_f$  and mean uniform density.

The expectation of the number of the pellet crossings after long period of time  $\Delta t$  is calculated as:

$$N_{cross} = P \frac{\Delta t}{T_{rev}} . \quad (1.8)$$

The probability  $P$  to cross the pellet during one revolution in the ring for given ion can be expressed as:

$$P = P_y P_x \quad (1.9)$$

where

$$P_y = \begin{cases} \frac{y_p}{h}, & \text{if } y_p < h \\ 1, & \text{if } y_p \geq h \end{cases} \quad (1.10)$$

is the probability to hit the pellet in vertical direction. The probability to cross the pellet in the horizontal direction  $P_x$  can be calculated as a ratio between the pellet flux cross-section and cross-section of the line along the ion trajectory at width of  $x_p$  (Fig.1.1).

Length of such a line along ion beam orbit  $H$  does not depend on the ion vertical co-ordinate, and depends on horizontal ion co-ordinate  $x_i$  as follows:

$$H = 2\sqrt{r_f^2 - (x_i - \Delta_p)^2} , \quad (1.11)$$

when  $-r_f < x_i < r_f$ , and equal to zero, when the ion co-ordinate is bigger than flux dimensions. Here  $\Delta_p$  is the horizontal displacement of the pellet flux centre from the ion equilibrium orbit.

$$P_x = \frac{H x_p}{\pi r_f^2} , \quad (1.12)$$

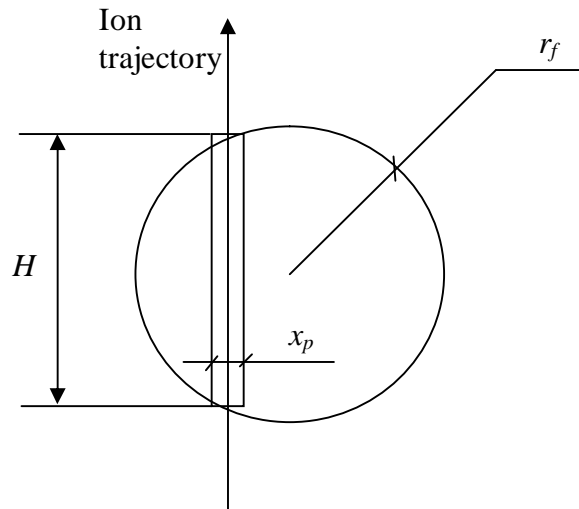


Fig. 1.1. The pellet flux cross-section by the horizontal plane.

During step of ion motion equation integration the ion oscillates in horizontal plane and the target length along the ion trajectory has to be averaged over the betatron oscillations. At given particle co-ordinates in the horizontal phase plane  $(x_i, x'_i)$ , its momentum deviation  $\Delta p/p$  and lattice parameters in the target position (alpha and beta function -  $\alpha_x, \beta_x$ , horizontal dispersion –  $D$  and its derivative  $D'$ ) the particle horizontal co-ordinate in the target position can be expressed by the following formulae:

$$\begin{aligned}
 x_i(\varphi) &= A_x \cos \varphi + D \frac{\Delta p}{p}, \\
 A_x &= \sqrt{I_x \beta_x}, \\
 I_x &= \beta_x x_\beta'^2 + 2\alpha_x x_\beta x_\beta' + \frac{1 + \alpha_x^2}{\beta_x} x_\beta^2, \\
 x_\beta &= x_i - D \frac{\Delta p}{p}, \\
 x_\beta' &= x_i' - D' \frac{\Delta p}{p}.
 \end{aligned} \tag{1.13}$$

Here  $\varphi$  is the phase of the betatron oscillations. The mean target length  $\langle H \rangle$  can be calculated as an integral:

$$\langle H \rangle = \frac{2}{\pi} \int_{\varphi_{\min}}^{\varphi_{\max}} \sqrt{r_f^2 - (x_i(\varphi) - \Delta_p)^2} d\varphi, \tag{1.14}$$

where  $\varphi_{\min} = 0$  and  $\varphi_{\max} = \pi$ , when the ion trajectory lies inside the pellet flux, or are calculated from elementary geometrical reasons:

$$\begin{aligned}
 \varphi_{\min} &= \arccos \left( \frac{\Delta_p + r_f - D \frac{\Delta p}{p}}{A_x} \right), \\
 \varphi_{\max} &= \arccos \left( \frac{\Delta_p - r_f - D \frac{\Delta p}{p}}{A_x} \right).
 \end{aligned} \tag{1.15}$$

When the number of the pellet crossings during time  $\Delta t$  is known, calculating the number of crossings for all modeling particles one can calculate luminosity in accordance with:

$$L = \frac{N_i}{N_{MP}} \frac{\mathfrak{R}l}{\Delta t} \sum N_{cross}, \tag{1.16}$$

where  $N_i$  and  $N_{MP}$  are the total number of ions in the ring and number of modeling particles,  $\mathfrak{R}$  is the pellet density,  $l$  is the mean pellet length along the ion trajectory.

## 1.2. Beam parameter variation

Investigation of the ion beam dynamics is performed with BETACOOOL code using multi particle simulation. In this algorithm the ion beam is presented by array of modeling particles. The heating and cooling processes involved into simulations lead to change of the particle momentum components and particle number, what is calculated in accordance with step of dynamics simulation over time.

Concerning to the pellet target, when the number of the pellet crossings during the step of dynamics simulation is known, the particle momentum variation after each crossing the pellet is calculated separately. Change of the transverse momentum components is related mainly with a multiple Coulomb scattering from nuclei of the target atoms. Change of the longitudinal momentum component takes a place due to ionization energy loss in interaction with electrons of the target atoms.

In the BETACOOOL the simulation of the ion momentum variation after single crossing a pellet is provided using Monte-Carlo method based on Urban model for the longitudinal degree of freedom and plural scattering model for the transverse ones. In the frame of the Urban model the total energy losses, calculated using Bethe-Bloch formula, are distributed between ionization and excitation events. The number of events has Poissonian distribution around expectation, the energy loss due to ionization are distributed from mean ionization energy to maximum transferable energy determined by kinematics of the process. The plural scattering model is based on generation of scattering angle in accordance with Rutherford cross-section for a screened Coulomb potential.

Probability of the particle loss after crossing a target is determined mainly by three processes: single scattering on large angles, charge exchange and nuclear reactions in the target. Cross-section of the single scattering on large angle is calculated in accordance with Rutherford formula. The charge exchange in the target in the present version of the program is taken into account only for fully stripped ions. For such an ion the program calculates cross-section of a capture of an electron in the target. For antiprotons particle losses due to charge exchange are not exist.

To simulate the variation of the ion momentum components the program calculates expectations for numbers of elementary events after single crossing the pellet, i.e. numbers of excitation and ionization of the target toms and number of scattering on the nuclei. Real number of events assumed to be distributed around its expectation in accordance with Poisson law. In each elementary event the momentum variation is calculated as a random number distributed in accordance with corresponding law.

## 1.3. Short time-scale luminosity variations

To distribute pellets along a tube before injection them into the beam the simple random generation method is used. Pellets are distributed normally in a long cylinder which has radius  $R_0$  equal to the flux radius (Fig.1.2). A longitudinal position of each pellets are calculated in accordance with mean distance between pellets  $L_0$  and dispersion of the longitudinal position  $D_L$  ( $D_L=0$  means that distance between all the pellets equals  $L_0$ ).

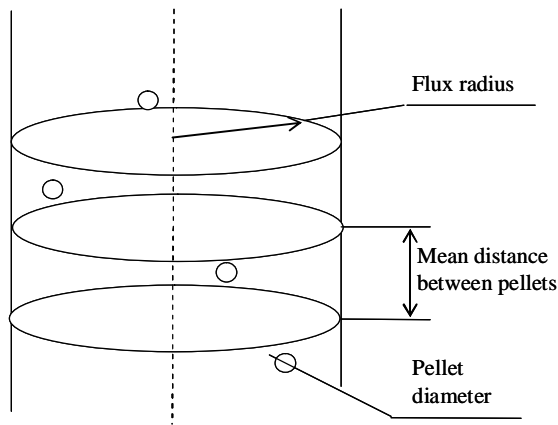


Fig 1.2. Pellets distribution along cylinder.

On Fig.1.3 real pellets flux distribution in generated by the BETACOOOL program is shown. On Fig.1.3a points are cross section of the pellet flux, on Fig.1.3b points are horizontal and vertical projections of the pellets.

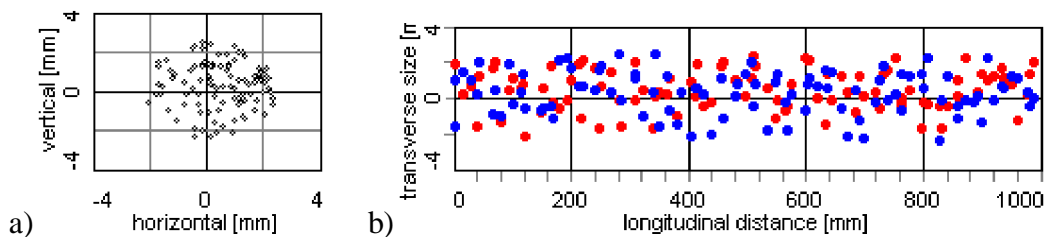


Fig. 1.3 Transverse cross-section (a) and longitudinal distribution of pellets (b): red – horizontal coordinate, blue – vertical.

Profile of the beam (which pellets are crossing) comes from a special algorithm of calculating beam dynamics under action of cooling and heating effects. As the first beam profile Gaussian distribution is used. Beam profile consists of two parts – horizontal and longitudinal profile (Fig.1.4).

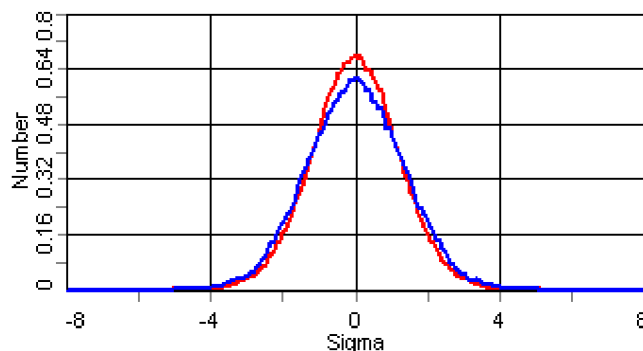


Fig. 1.4. Beam profiles

On Fig.1.4 two kinds of the beam transverse profiles are shown. Red line is horizontal profile and blue one is vertical. The beam profiles are presented in the units of rms value.

When pellets are generated and distributed in all over a cylinder the main algorithm start working. Algorithm begins moving pellets in vertical direction from the top to the bottom with defined step.

For better understanding the process of luminosity calculation is illustrated by the Fig.1.5. Points on the picture are the pellets that come through the beam profile (red line – beam horizontal profile, blue one – beam vertical profile). When pellet crosses the beam, corresponding beam profiles meanings multiplies on each other and results are summing up for each pellet then. As a result *relative luminosity in arbitrary units* is turned out.

On each step “weight” value  $P_{xy}$  for each pellet is calculated. Pellet “weight” value means multiplying of the horizontal and vertical beam profiles meanings where the pellet crosses the beam. To find the pellet “weight” value the algorithm recalculates ones coordinates to the corresponding value of horizontal and vertical beam profiles and multiplies them on each other.

$$P_{xy} = P_x \cdot P_y . \quad (1.17)$$

In this formula  $P_x$  - horizontal beam profile value in the place where pellet crosses the beam. Accordingly,  $P_y$  - vertical beam profile value. If pellet is not in the beam area  $P_{xy}$  is equal to zero. So then weight values from all pellets are summing up (1.17). And algorithm makes new step.

$$P = \sum_{i=n} P_{xy_i} , \quad (1.18)$$

$P_{xy_i}$  - “weight” value of the  $i$  pellet,  $n$  – number of pellets that are in the flux.

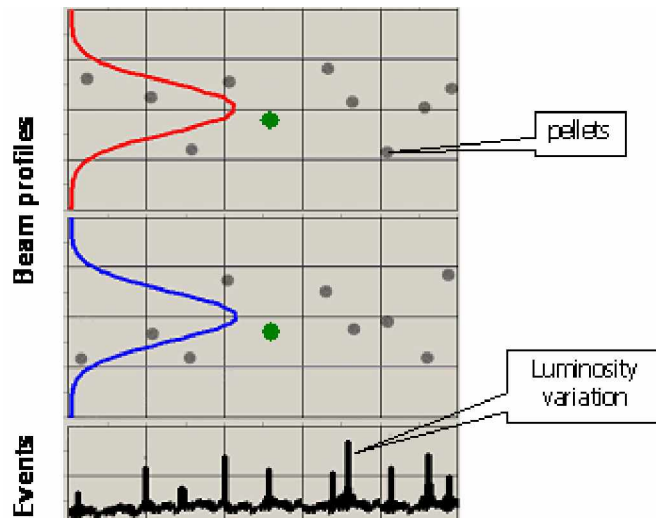


Fig. 1.5. Pellet target luminosity variations

#### 1.4. Effective luminosity

If the detector is designed with luminosity limit it will be overloaded by short-scale luminosity variations. The problem of the effective luminosity calculation exists due to fact that the evolution of beam parameters have to be calculated for the large number of the turns in the long-time scale, but the calculation of the real interaction of particles with pellets can be calculated in short-time scale only.

To avoid this problem one can calculate the short-scale luminosity variation (Fig.1.6) on each integration step of the long-scale luminosity evolution (Fig.1.7). We can assume that the arbitrary average value of short-scale signal from pellets (blue line on Fig.1.6) corresponds to the average luminosity of the long-scale value (blue line on Fig.1.7) which is calculated in accordance with (1.4).

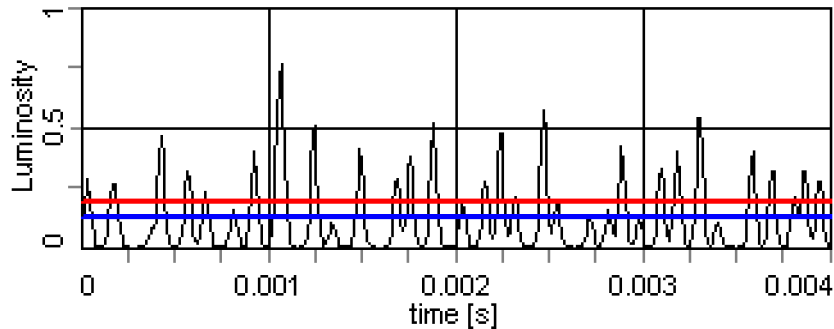


Fig. 1.6. Short-scale signal from pellets: blue line – average value, red line – detector limit.

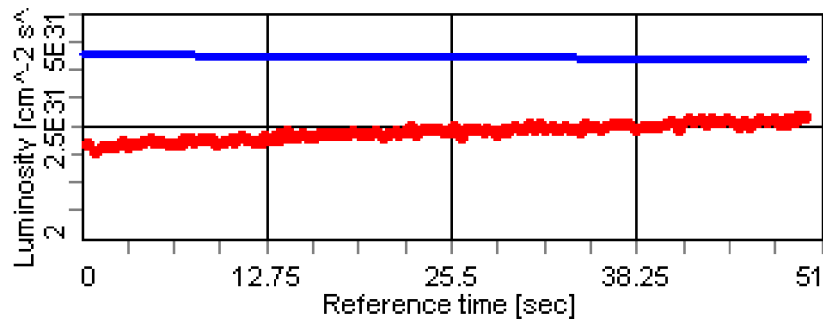


Fig. 1.7. Long-scale luminosity evolution on time (blue line) and effective luminosity for “top cut” model of detector limit (red line).

Also we can introduce the detector limit level (red line on Fig.1.6) which corresponds to the maximum acceptable luminosity for the certain detector design. In these simulations we consider two ultimate variants of the detector limit: the luminosity value is saturated and equal to the detector limit (“top-cut” model on Fig.1.8), the detector is completely overloaded and can not accept any events - luminosity value is zero (“full-cut” model on Fig.1.8). The real detector design can be placed between these two ultimate cases.

The total integral of pellet signal (Fig.1.8a) corresponds to average luminosity (Fig.1.7, blue line). The effective luminosity in the case of the detector limit can be calculated with following expression:

$$L_{eff} = L_{aver} \frac{I_{cut}}{I_{aver}} \quad (19)$$

where  $L_{aver}$  – average luminosity in the long-scale algorithm (Fig.1.7, blue line),  $I_{aver}$  – integral of the total pellet signal (Fig.1.8a),  $I_{cut}$  – integral of pellet signal for different detector limit (Fig.1.9b,c). An example of the effective luminosity for PANDA parameters is presented on Fig.1.7 (red line) for the “top-cut” model of the detector limit.

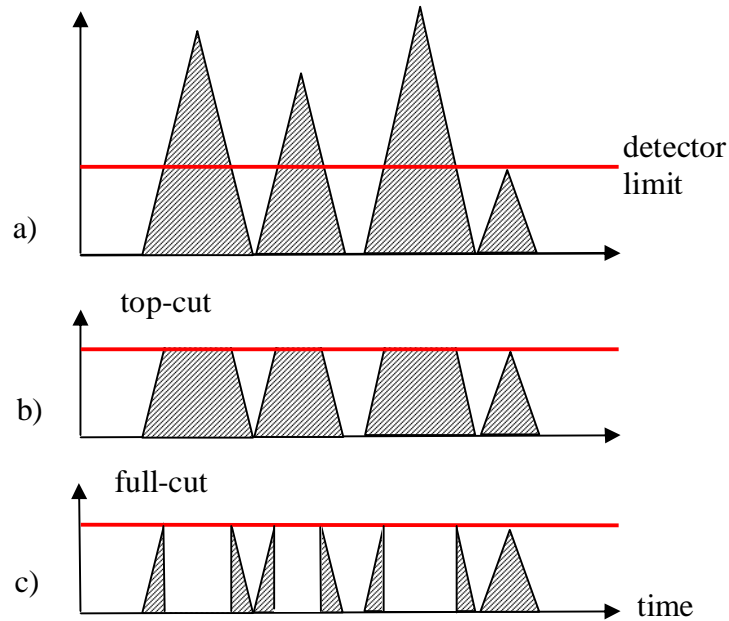


Fig.1.8. Two models of detector limit.

## 2. WASA experiment

### 2.1. Experimental conditions

For the benchmarking of the luminosity variations algorithm in BETACOOOL program the data analysis of the experiment with the internal target WASA at COSY storage ring (FZJ, Juelich, Germany) was used. Parameters of this experiment [4] are presented in Table 2.1.

Table 2.1. Main parameters of WASA@COSY

<b>Deuterium beam</b>	
Momentum, GeV/c	1.2
Energy, MeV/u	177
Particle number	$2 \times 10^{10}$
<b>Deuterium target</b>	
Pellet radius, $\mu\text{m}$	15
Pellet flux radius, mm	2.5
Mean distance between pellets, mm	10
Deuterium density, $\text{atom}/\text{cm}^{-3}$	$6 \times 10^{22}$
Mean target density, $\text{cm}^{-2}$	$2 \times 10^{15}$

Conditions of the experiment had two peculiarities. The first one is a decreasing of vacuum quality parameter in the pellet target station area. On the Fig.2.1 the storage ring vacuum distribution is shown. The area with high histogram meanings indicates low vacuum quality near the pellet target station. Such vacuum loss can be explained by the pellet collector problem. It can not catch all pellets up and they are deflecting from the collector. The evaporation of the pellet significantly decreases the vacuum condition around the target station area.

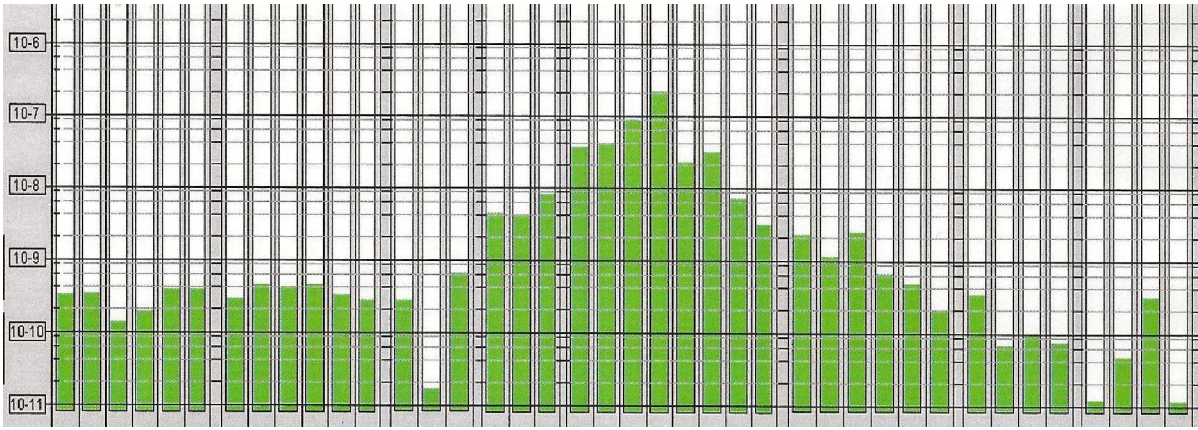


Fig. 2.1. COSY vacuum conditions

The second one is consisted on the pellet flux time unhomogeneity. The pellet flux is taken aside by a special valve before the injection cycle is started. After finishing the injection the valve takes its normal position and pellet flux comes to the beam centre. Such procedure is applied to increase beam life time and leads to pellet flux heterogeneity pointed below. Gradual pellet target luminosity increasing is shown on Fig.2.2. As one can see in the area pointed as (a) the luminosity grows up first and fall down after some maximum value because of the beam particles number getting smaller. Experimentally was found out that such luminosity growing has place to be because of the valve. On the area (b) pellet target luminosity without using the valve is shown. As ones can see there is no luminosity increasing in the beginning of working cycle. Yellow and green lines are signals from pellets which come from pellet generator (yellow line) to the beam area (green line). Black line shows number of particles in the beam. Other lines are signals from different detectors.

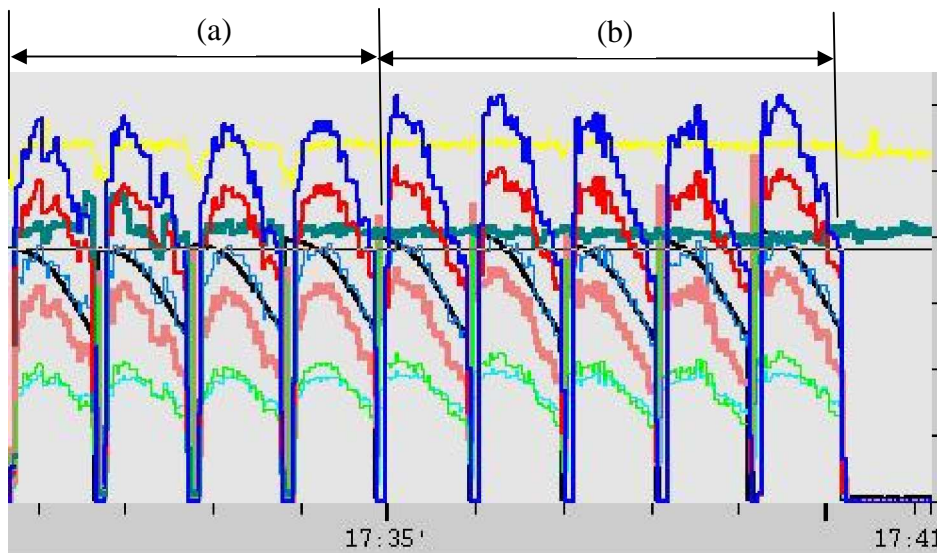


Fig. 2.2. Pellet target luminosity. (a) - with valve, (b) - without valve

## 2.2. Comparison of experimental and simulation results

At the frame of COSY experiments two storage ring working schemes were applied and numerically modeled: RF switched off and RF switched on (barrier bucket mode). Initially the mode without barrier bucket was used to verify the numerical model. The results of measurements are presented on the Fig.2.3. One can see long trace cut at the end (bottom of the picture). This reflects a displacement of beam mean energy. Cutting of the trace can be explained by longitudinal

acceptance limitation. Profile of the beam which is shown inside a circled area of the picture is displaced from the centre and cut from the left.

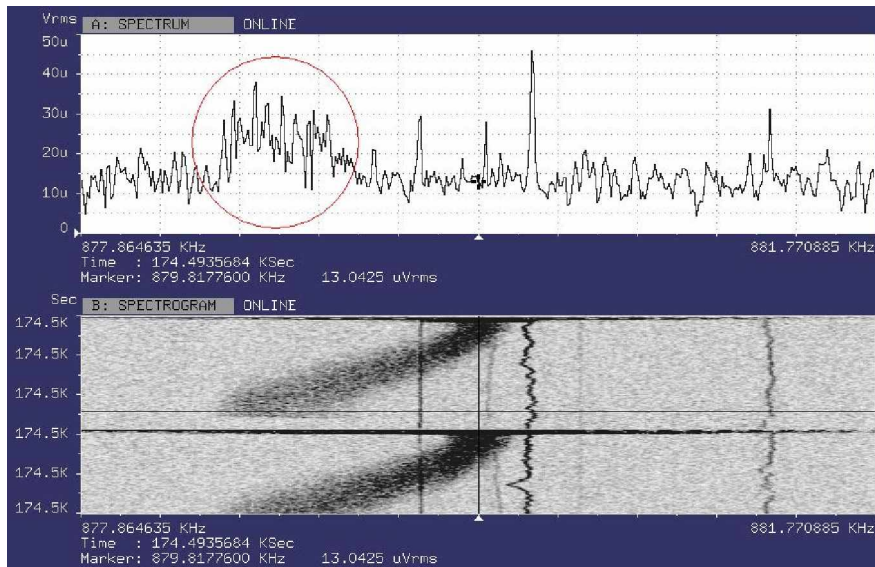


Fig.2.3. The COSY beam displacement. Burier bucket is switched off.

On the Fig.2.4 BETACOOOL modeling of the beam energy decreasing is presented. Relative momentum shift corresponds to about 4 «sigma», the sigma in the plot is equal to initial momentum spread.

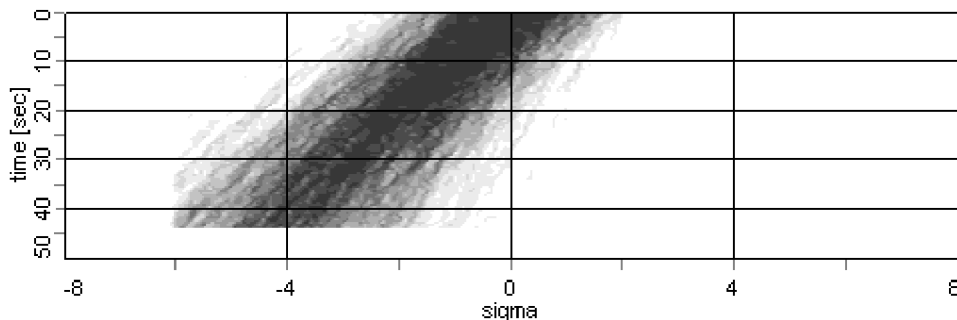


Fig. 2.4. Simulation of the momentum spread evolution. Burier bucket is switched off.

To compare this result with experiment data one needs to calculate the momentum shift from the Fig.2.4 in accordance with the formula:

$$\frac{\Delta p}{p} = \frac{1}{\eta} \frac{\Delta_f}{n f_0}; \quad (20)$$

Here  $f_0 = 879.82$  kHz is initial revolution frequency,  $\Delta_f = 0,977$  kHz is the frequency shift of the distribution centre,  $n=1$  is the harmonic number. The formula (20) gives momentum shift  $8.1 \times 10^{-4}$  that is a good agreement with the simulation.

The particle distribution on momentum deviation obtained in the simulations (Fig.2.5) reproduces the shape of the beam Schottky spectrum measured in the experiment (circled curve at the upper plot in Fig.2.3).

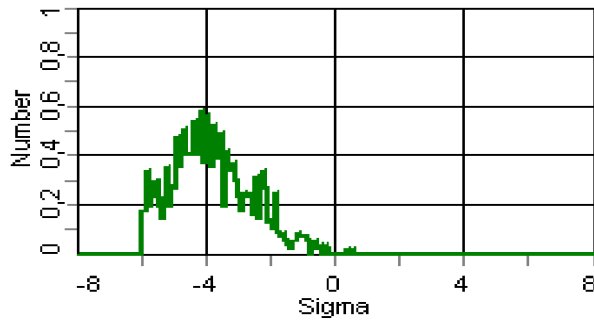


Fig.2.5. The simulated beam profile after 40 sec of the experiment.  
Burier bucket is switched off.

When the burier bucket is switched off particle loses are very fast. On COSY one third of all particles are lost by 46 seconds. A result of the particle loses modeling by BETACOOOL code is presented on the Fig.2.6 which has a good agreement with experiment (Fig.2.2). The good agreement between simulations and experiment tells that the pellet target parameters and effective target density are fitted correctly.

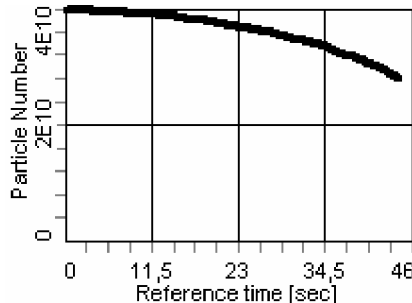


Fig.2.6. Particle loses modeling (barrier bucket off).

The second working scheme is when *the burier bucket is switched on*. Applying of the barrier bucket makes particle loses more slowly. In this case loses on the longitudinal acceptance is observed. As it is shown on the Fig.2.7 (black line) one third of all particles in storage ring are lost for about 70 seconds. When the barrier bucket is switched on the RF noise does not permit to measure Schottky noise spectrum like on Fig.2.3.

On the Fig.2.7 signals from storage rings detectors are presented: black line shows particle number in the storage ring, yellow and green lines corresponds to the pellet number, other colors lines are count rate values from different detectors which are proportional to the luminosity value.

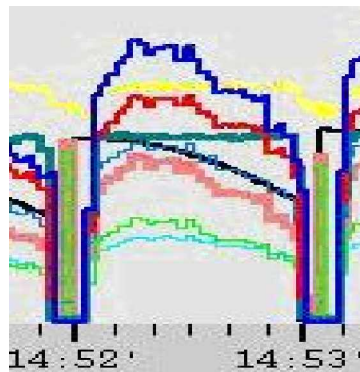


Fig.2.7. Particle loses (black line). Burier bucket is switched on

On the Fig.2.8a the BETACOOOL modeling of the particles number is presented as a function of time. As example of BETACOOOL modeling opportunities luminosity modeling picture is

presented (Fig.2.8b). Simulation results have a good agreement with experimental results on Fig.2.7.

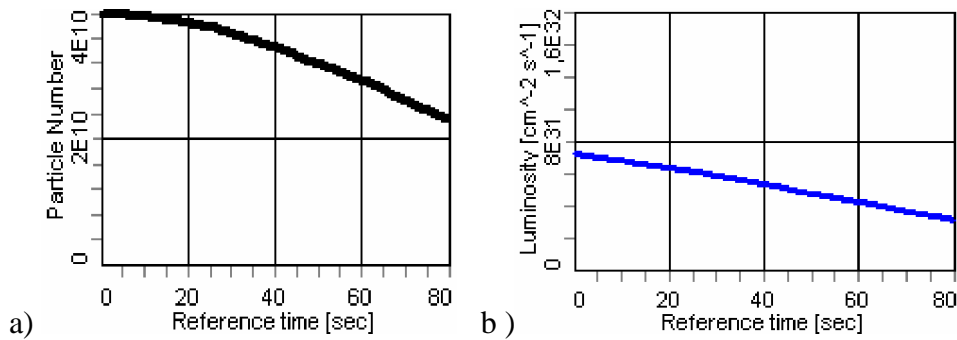


Fig. 2.8. Simulation of particle losses (a) and luminosity dependence (b) on time. Burier bucket is switched on

Result of the short-scale algorithm for COSY parameters is shown on the Fig.2.9a. Here one can see relative luminosity variations in time. Results of the short-time scale simulation of the luminosity variation are in a good agreement with experimental measurements at COSY (Fig.2.9b).

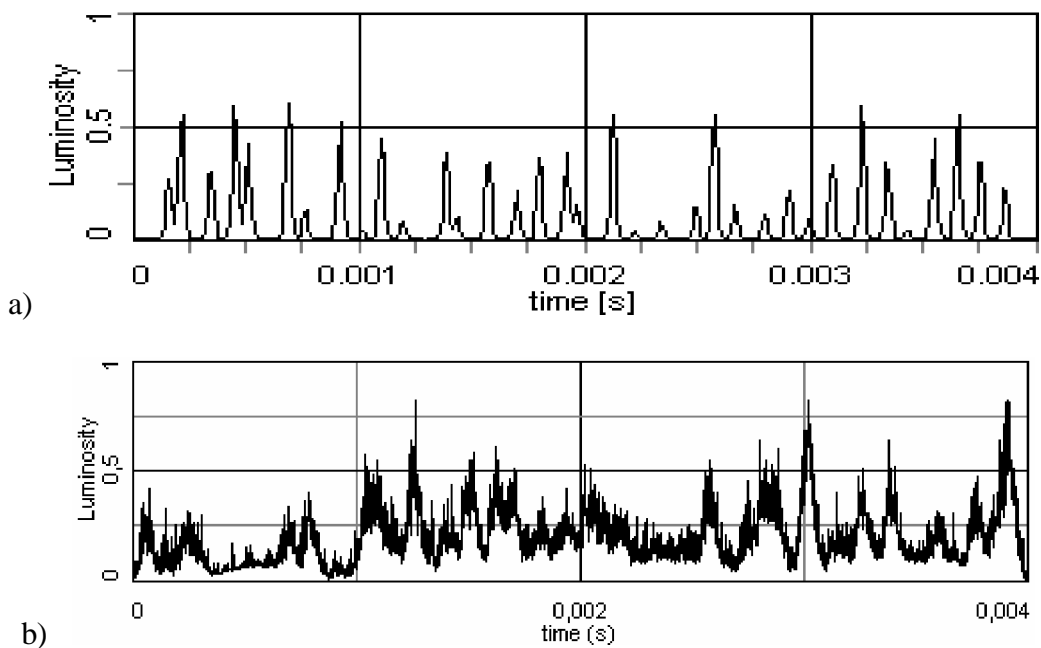


Fig.2.9. Pellet target luminosity variations on WASA@COSY: a – simulation, b – experiment.

### 3. Simulation of PANDA experiment

The numerical simulation of the effective luminosity was done for two operation regimes of the PANDA experiment with high-luminosity (HL) and high-resolution (HR) modes. The typical parameters of the pellet target and antiproton beam are presented in Table 3.1.1

Table 3.1.1 The typical parameters of PANDA experiment

<b>Pellet target</b>		
Hydrogen density, atom/cm <sup>3</sup>	4,26×10 <sup>22</sup>	
Pellet size (diameter), mm	0,028	
Pellet flux radius, mm	1,25	
Distance between pellets, mm	5	
Effective target density, cm <sup>-2</sup>	4×10 <sup>15</sup>	
<b>Antiproton beam</b>		
Beam energy, GeV	8	
Operation mode	HR	HL
Particle number	10 <sup>10</sup>	10 <sup>11</sup>
Momentum spread	10 <sup>-5</sup>	10 <sup>-4</sup>
<b>Mean luminosity, cm<sup>-2</sup>s<sup>-1</sup></b>	2×10 <sup>31</sup>	2×10 <sup>32</sup>

The effective luminosity is ratio of the registered event number by the detector to the total event number of antiproton interactions with pellets. The dependence of the effective luminosity on the pellet size in micrometers for the different detector limit is presented on Fig.3.1 (HR) and Fig.3.2 (HL). The detector limit was chosen in the range from the value of the mean luminosity to the value in 10 times larger. The distance between pellets was chosen in accordance with the pellet size to keep the same effective target density.

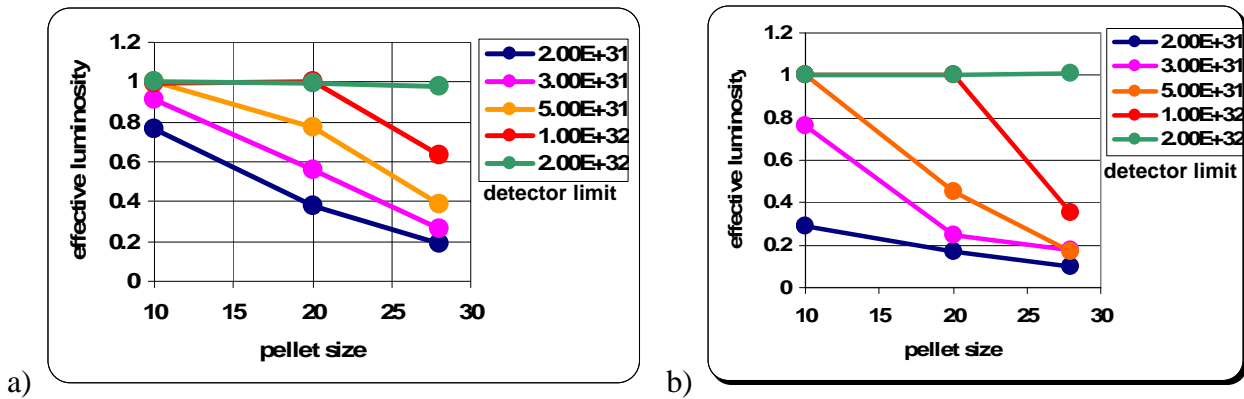


Fig.3.1. Effective luminosity simulation for different limit of detector (high resolution mode). a) “top-cut” model, b) “full-cut” model.

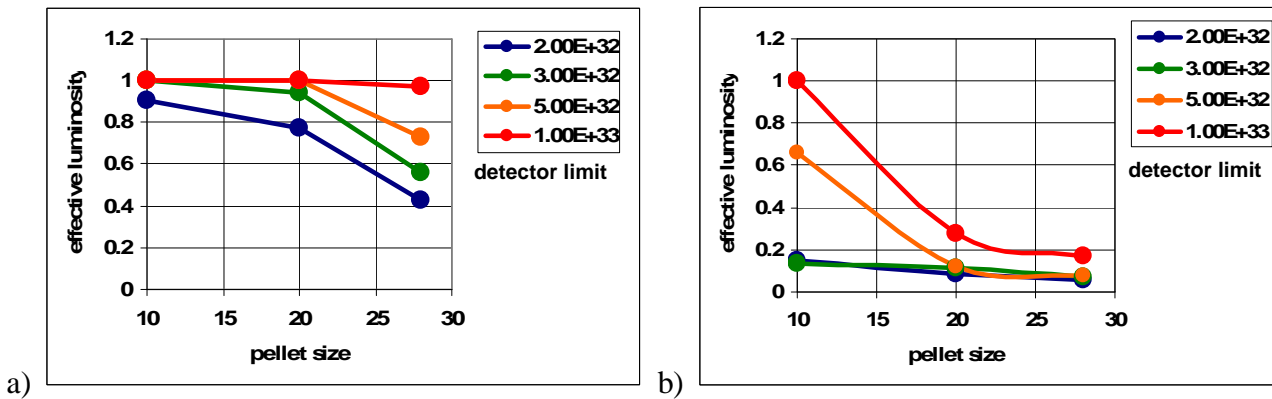


Fig.3.2. Effective luminosity simulation for different detector limit (high luminosity mode). a) “top-cut” model, b) “full-cut” model.

Simulation results show that for the HR mode the effective luminosity equal to the mean luminosity if the detector limit is defined by the mean luminosity for the HL mode  $2 \times 10^{32} \text{ cm}^{-2} \text{ s}^{-1}$ . A reduction of the effective luminosity for the HR mode can exist if some detectors will be designed especially for the HR mode and the detector limit will exceed the mean luminosity in two times only.

In the case of the HL mode the effective luminosity is rather difference for “top-cut” and “full-cut” models. For the “top-cut” model the maximum pellet size has to be less than  $20 \mu\text{m}$  if the detector limit exceeds the mean luminosity in two times only. For the “full-cut” model the pellet size has to be less than  $10 \mu\text{m}$  and detector limit is sufficiently higher than  $2 \times 10^{33} \text{ cm}^{-2} \text{ s}^{-1}$ .

## Conclusion

The comparison of simulations and experiments with the internal pellet target WASA@COSY shows a good agreement. A new algorithm for short-time process of the luminosity variation was implemented in the BETACOOOL code and was benchmarked with the experiments at COSY. This new algorithm is being developed for the effective luminosity simulation when peak to mean luminosity ratio can reach a big value unacceptable for detector.

Simulation results show that for the high resolution mode the effective luminosity can be equal to the mean luminosity if the pellet size will be less than  $20 \mu\text{m}$  and all detectors will be designed for the maximum luminosity value  $2 \times 10^{32} \text{ cm}^{-2} \text{ s}^{-1}$  which is corresponds to the high luminosity mode. For the high luminosity mode the pellet target can be used for the detector design with “top-cut” mode only. The detector design with “full-cut” mode can not be used for the high luminosity mode due to very large reduction of the effective luminosity.

## Reference

- [1] The PANDA experiment at FAIR. GSI Scientific Report 2004. <http://www-panda.gsi.de>
- [2] D.Prasuhn, U.Bechstedt, J.Dietrich, et al. Status of The Cooler Synchrotron COSY Juelich. Proceedings of the 2001 Particle Accelerator Conference, Chicago.
- [3] A. Sidorin, I. Meshkov, I. Seleznev, A. Smirnov, E. Syresin, A. Smirnov, and G. Trubnikov. BETACOOOL program for simulation of beam dynamics in storage rings. Nucl. Instrum. Methods, A, **558**, 325 (2006). <http://lepta.jinr.ru>
- [4] A. Smirnov, A. Sidorin, D. Krestnikov, R. Pivin, D. Prasuhn, M. Wolke. Simulation of Pellet Target Experiments with Betacool Code. Proceedings of RuPAC 2008, Zvenigorod, Russia. <http://jacow.org>